

Received March 23, 2020, accepted April 1, 2020, date of publication April 6, 2020, date of current version April 22, 2020.

Digital Object Identifier 10.1109/ACCESS.2020.2985993

# Biodegradable Piezoelectric Transducer for Powering Transient Implants

SOPHIA SELVARAJAN<sup>1,2</sup>, ALBERT KIM<sup>3</sup>, (Member, IEEE), AND SEUNG HYUN SONG<sup>1</sup>

<sup>1</sup>Department of Electronics Engineering, Sookmyung Women's University, Seoul 04310, South Korea

<sup>2</sup>Department of Biophysics, Institute of Quantum Biophysics (IQB), Sungkyunkwan University (SKKU), Suwon 16419, South Korea

<sup>3</sup>Department of Electrical and Computer Engineering, Temple University, Philadelphia, PA 19122, USA

Corresponding authors: Albert Kim (albertkim@temple.edu) and Seung Hyun Song (shsong.ee@sookmyung.ac.kr)

This work was supported by the Sookmyung Women's University Research under Grant 1-1803-2021.

**ABSTRACT** Transient implantable medical devices based on biodegradable electronics can be used for diagnostic and therapeutic purposes for a desired duration and undergo biodegradation, unlike their conventional counterparts. However, powering transient implants through biodegradable power sources remains underexplored. Here, we report biodegradable piezoelectric transducer fabricated using 0-3 composite film made of barium titanate nanoparticles and poly (L-lactic-co-glycolic) acid polymer (BT-PLGA). The proposed BT-PLGA can be utilized in two different powering schemes; ultrasonic powering and energy harvesting from low frequency acoustic waves. We demonstrated that the power density of the BT-PLGA transducer can reach up to 10 mW/cm<sup>2</sup> in ultrasonic powering. The energy harvesting from low frequency acoustic waves could also readily generate sufficient power for small electronics. The fabricated transducers underwent complete biodegradation in physiological conditions within 100 days. The development of the biodegradable piezoelectric transducer potentially provides a reliable power source for transient implants, especially for deeply seated bioelectronics. The output performance, biocompatibility, and tunable biodegradation of BT-PLGA transducer demonstrate its potential as a biodegradable power source for transient implantable devices.


**INDEX TERMS** Biodegradable materials, implants, piezoelectric transducers, wireless power transmission.

## I. INTRODUCTION

Transient electronics refer to the electronic systems that are devised using bioresorbable or biodegradable materials, which are designed to be dissolved in biofluids after a desired operation lifetime [1]–[5]. Major benefits from transient electronics technology include the elimination of the secondary surgery to remove the implanted devices, reduction of the electronic waste, and prevention of sensitive data leakage [2], [6]. The advancements in transient electronics have led to the developments of many transient implants; examples include force sensors to measure physiological pressure [7], nerve stimulator [8], electrophysiological sensors [3], neural mapping device [9], and biosensors [10]–[14]. Although significant advancements in transient electronics technology with respect to diagnostics and therapeutics have been made, the development of biodegradable power supply remained a

missing link as most of these implants depend on reliable power sources for their functions [15], [16]. In a conventional scenario, batteries can serve this purpose [17], but they are not usually biocompatible and have to be replaced by surgery, which partially negates the advantages of transient devices [18]. Hence, developing transient power sources that can operate for a stable period of time alongside the implants is the need of the hour [15].

Naturally, transient power sources for different powering schemes have been developed. For instance, glucose fuel cells with a stable operation period of about ~100 days and the power density ranging from 2.5 to 8  $\mu\text{W}/\text{cm}^2$  were demonstrated [19]. An inductive power transfer using a bioresorbable inductor also successfully operated a transient neural stimulator [8]. Harvesting energy available within the body is another attractive alternative. For example, bioabsorbable triboelectric nanogenerators were demonstrated with a power density of 2.16  $\mu\text{W}/\text{cm}^2$  with an excellent biocompatibility [20], [21]. In addition,

The associate editor coordinating the review of this manuscript and approving it for publication was Masood Ur-Rehman .

bioresorbable capacitors, another critical element in power storage, were demonstrated with a power density in the order of  $1 \text{ mW/cm}^2$  [22], [23].

However, acoustic (ultrasound) powering has remained under-explored because biodegradable piezoelectric transducers have not yet been developed, despite the fact that it is suitable for powering implantable devices due to a long powering distance and minimal heating of tissues (under the FDA limit for the imaging applications) [24]–[28]. Additionally, the powering efficiency using ultrasound, especially in the case of small deeply seated implants [26], [29], can be greater than other wireless powering schemes. Thus, biodegradable piezoelectric transducers operated through acoustic (ultrasound) power transfer technology are highly promising for powering transient implants.

In this work, we demonstrate a biodegradable piezoelectric transducer that can potentially be utilized to power transient implants. The transducer is a 0-3 composite film made of barium titanate (BT) nanoparticles and poly (L-lactico-glycolic) acid (PLGA) polymer. BT is a biocompatible perovskite piezoelectric material with the  $d_{33}$  coefficient of  $\sim 100 \text{ pC/N}$  [30]–[32]. PLGA is an FDA approved biodegradable polymer, extensively used in constructing biomedical implants; hence we chose PLGA as the polymer material for the piezoelectric composite. We demonstrate that the BT-PLGA transducer can be used in ultrasonic powering as well as harvesting energy from low-frequency acoustics. The maximum power generated by the BT-PLGA transducer was  $1 \text{ mW}$ , which is more than sufficient to power implantable devices such as pacemakers ( $\sim 1$  to  $10 \text{ }\mu\text{W}$ ) and neurostimulator ( $\sim 10$  to  $100 \text{ }\mu\text{W}$ ) [24], [33].

## II. RESULTS & DISCUSSIONS

### A. DESIGN AND FABRICATION OF BIODEGRADABLE PIEZOELECTRIC TRANSDUCER

Our proposed scheme of the biodegradable piezoelectric transducer for transient implants is described in Fig. 1. A transient implant for various applications (e.g. sensing, actuation, stimulation, drug delivery, etc.) can potentially be powered through the biodegradable piezoelectric transducer converting incoming ultrasound applied from an external transducer or low-frequency vibrations generated inside of human body (e.g., blood flow) into electrical power (Fig. 1a). After operating for the intended lifetime of the device, the entire implant, including the biodegradable transducer, can undergo complete biodegradation without the implant extraction (Fig. 1b).

The biodegradable piezoelectric active material was a 0-3 composite consists of BT nanoparticles embedded in a PLGA film. 0-3 composite piezoelectric material refers to isolated (i.e. the zeroth order connectivity) patches of piezoelectric materials (e.g. BT nanoparticles) encapsulated in a polymer network with the third order connectivity [34]. Although the piezoelectric performances of 1-3 or 2-2 composites are superior to those of 0-3 composites [35], the degradation kinetics of 0-3 composite are expected to be homogeneous as the embedded BT nanoparticles are released

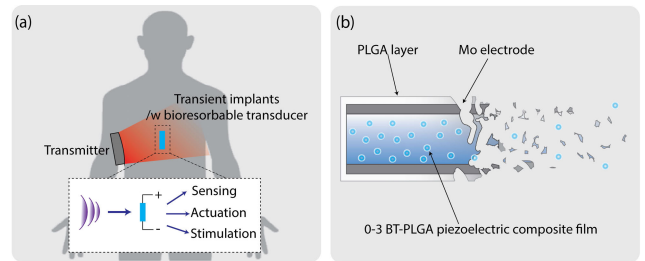


**FIGURE 1. Concept and design of BT-PLGA transducer: (a) Overall concept of the proposed work; a 0-3 composite piezoelectric BT-PLGA transducer can serve as a power source for transient implants, harvesting energy from acoustic waves. (b) The transducer can undergo biodegradation after a desired operation duration.**

from the PLGA encapsulation during degradation. For electrical connections, molybdenum (Mo), biocompatible and biodegradable, was used as the electrode material. The final device was then encapsulated in another layer of PLGA (Fig. 1b).

As the first step of the device fabrication, BT nanoparticles were synthesized using the hydrothermal method using titanium dioxide ( $\text{TiO}_2$ ) and barium chloride ( $\text{BaCl}_2$ ) as precursors. The precursors were dissolved in  $10 \text{ M NaOH}$  solution with 1:10 molar ratio of  $\text{TiO}_2$  and  $\text{BaCl}_2$ . The solution was then transferred into a Teflon-lined autoclave (80% volume of the autoclave was filled) and treated at  $200 \text{ }^\circ\text{C}$  for 72 h. After the solution was cooled down to room temperature, the resulting particles were washed several times with distilled water by centrifuging at 6,000 rpm for 20 minutes until neutral pH was attained. The resulting pellet was dried overnight in a convection oven at  $80 \text{ }^\circ\text{C}$ . The piezoelectric tetragonal phase of the BT nanoparticles was confirmed by Raman spectroscopy ( $532 \text{ nm}$ ,  $20\times$  objective,  $1 \text{ mW}$ , Alpha-300a, WiTec, Germany). The Raman spectrum (Fig. 2a) shows the characteristic peaks at  $306 \text{ cm}^{-1}$  ( $A_1$  mode) and  $514 \text{ cm}^{-1}$  ( $B_1$  mode), which confirm the presence of  $\text{Ti}^{4+}$  ions in the parent lattice [36]. The scanning electron microscopy (JSM-7600F, JEOL, Japan) was used to characterize the sizes of the BT nanoparticles. A representative SEM image (Fig. 2b) shows the cubic shaped nanoparticles with average dimension of  $200 \text{ nm}$ .

The piezoelectric composite films with four different BT nanoparticle concentrations of 0, 10, 20, and 30 w/v% were fabricated into desired dimension of  $1 \text{ cm} \times 1 \text{ cm}$ . BT nanoparticle concentrations were controlled by varying the amount of BT nanoparticles added to a PLGA (lactic to glycolic mole percentage ratios of 50/50, Sigma Aldrich, USA) solution in chloroform with a concentration of  $100 \text{ mg/ml}$ . To obtain a homogeneous mixture, the solution was mixed using an ultrasonic homogenizer for 1 hour. The mixture was then solvent casted into a polytetrafluoroethylene (PTFE) mold followed by a vacuum drying step (room temperature, 3 days). The 0-3 BT-PLGA composite piezoelectric films was then removed from the mold (Fig. 3a). Electrical connections were made by attaching the Mo electrodes ( $25 \text{ }\mu\text{m}$  thick,  $\geq 99.9\%$ , Sigma Aldrich,

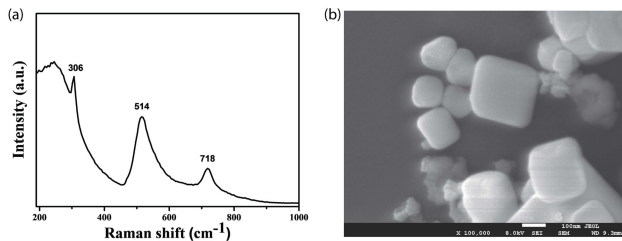


**FIGURE 2.** Characterization of synthesized BT nanoparticles: Representative (a) Raman spectrum confirming the tetragonal phase of BT and (b) SEM image of BT nanoparticles.

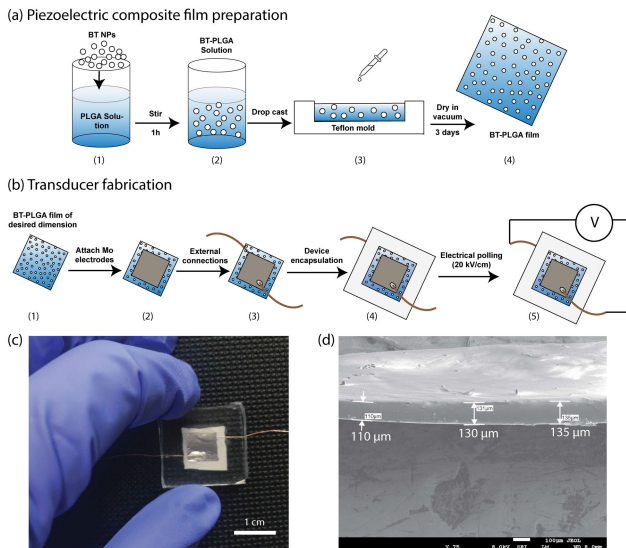


**FIGURE 3.** Schematics of BT-PLGA transducer fabrication process: (a) BT-PLGA composite film fabrication process, (b) BT-PLGA device fabrication, (c) optical photograph of fabricated transducer, and (d) cross-sectional SEM image of BT-PLGA composite film.

USA) and wires; wires were attached to the Mo electrode using silver paste. Afterwards, the transducer was encapsulated in another layer of PLGA for device passivation (Fig. 3b). Lastly, the transducer was electrically polled under the electric field of 200 kV/cm using a high-voltage source (Bertan 230, Spellman, USA). The fabricated 30 w/v% BT-PLGA with an active area of 1 cm × 1 cm is shown in Fig. 3c. The resulting films had thickness of ~ 120 μm (Fig. 3d).

**B. BT-PLGA TRANSDUCER FOR ULTRASONIC POWERING**

The fabricated BT-PLGA transducers were characterized for ultrasonic powering. The schematic depiction and the photo of the experimental setup are shown in Fig. 4(a). An external transducer (Mida Technology, USA) was attached to one end of the water tank and was driven in pulsed mode (freq. = 2.3 MHz, number of pulse = 10, repetition freq. = 10 kHz) via a function generator (AFG1022, Tektronix, USA) and a power amplifier (240L, ENI, USA). The BT-PLGA transducer was placed at the opposite end of the water tank about 10 cm from the transducer using a 3D printed fixture; the

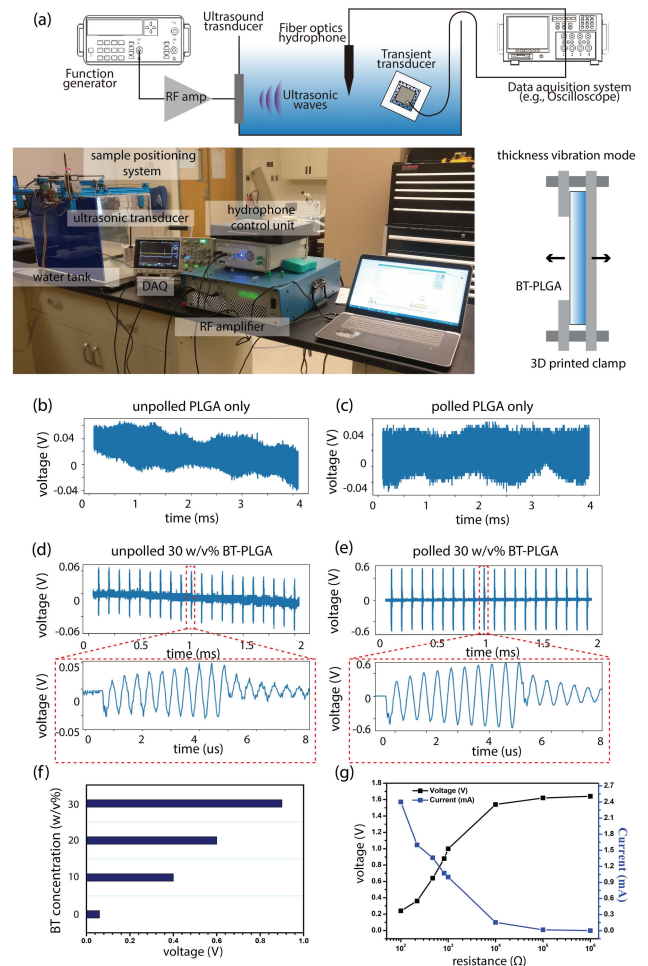


**FIGURE 4.** Ultrasound powering of BT-PLGA transducer: (a) experimental setup for ultrasonic powering and the vibration mode of the BT-PLGA transducer (b-c) piezoelectric output voltages of unpolled and polled PLGA transducers when stimulated by pulsed ultrasound generated from PZT transducer at a frequency of 2.3 MHz and 65 mW/cm<sup>2</sup> acoustic power intensity (d-e) piezoelectric output voltages of unpolled and polled 30 w/v% BT-PLGA transducers; the zoomed in views show the pulse train (f) Dependence of output voltages and BT loading concentrations of BT-PLGA transducer (0, 10, 20, and 30% w/v), and (g) Dependence of output voltage and output current of BT-PLGA transducer (30% w/v) on external load resistances (100 Ω to 1 MΩ).

back side of the BT-PLGA transducer was rigidly clamped to the acrylic support making the vibration mode of the transducer to be in the thickness mode (Fig. 4a). Using a fiber optics hydrophone (Precision Acoustics, UK), we measured the acoustic intensity. The hydrophone was placed in front of the BT-PLGA transducer to measure the acoustic intensity at the surface of the transducer; then the hydrophone was removed prior to the power characterization. The measured voltage amplitude of the hydrophone ( $V_{hp}$ ) was 6.5 mV. At 2.3 MHz, the hydrophone sensitivity ( $S_{hp}$ ) was about 150 mV/MPa. Thus, the peak pressure ( $p_{peak}$ ) was then obtained by dividing the hydrophone output by the sensitivity (equ. 1). The acoustic intensity was calculated based on the measured peak pressure using equ. 2, which yielded 65 mW/cm<sup>2</sup>. (I: acoustic intensity,  $p_{peak}$ : peak pressure [Pa],

$\rho$ : density of water [kg/m<sup>3</sup>],  $c$ : speed of sound in water [m/s])

$$P_{peak} = \frac{V_{hp}}{S_{hp}} [MPa] \quad (1)$$

$$I = \frac{P_{peak}^2}{2\rho \cdot c} [W/m^2] \quad (2)$$

Fig. 4(b)-(e) show the representative electrical outputs (directly connected to an oscilloscope with an input impedance of 1 M $\Omega$ ) of the BT-PLGA transducers with two different BT nanoparticle concentrations of 0 and 30 w/v%. The voltage outputs of the PLGA devices (i.e., 0 w/v%) under ultrasonic waves was within the noise level for both unpolled and polled devices (Fig. 4(b-c)). On the other hand, small voltage outputs ( $V_{pp} < 100$  mV) were measured from unpolled 30 w/v% BT-PLGA transducer; the zoomed view (indicated by the red dashed box) of the pulse clearly exhibited the sinusoidal outputs under the ultrasonic excitation (Fig. 4d). This performance of the BT-PLGA was enhanced by more than a factor of 10 after polling (1  $V_{pp}$ ) as shown in Fig. 4(d). Moreover, a monotonic increase in the output voltages under ultrasonic excitation was observed with increasing BT concentrations (Fig. 4(f)), indicating that the BT nanoparticles are responsible for the piezoelectric properties of the biodegradable BT-PLGA transducer.

To investigate the effective electric power of the BT-PLGA transducer, the load resistances were varied from 100  $\Omega$  to 1 M $\Omega$ . As shown in Fig. 4(g), output voltage increased gradually as the load resistance was increased, whereas the instantaneous current exhibited the opposite trend. The optimal load resistance was around 1 k $\Omega$ , where a maximum power of 1 mW was reached under a mild ultrasonic irradiation (65 mW/cm<sup>2</sup>). Given that the FDA limit of ultrasonic intensity for imaging applications is around 720 mW/cm<sup>2</sup>, we expect that a power density up to 10 mW/cm<sup>2</sup> can be achieved under higher intensity ultrasonic irradiation.

In addition to its function as the receiver for the ultrasonic powering, we explored the inverse piezoelectric effects of the BT-PLGA transducer, which can be used for different applications such as sonocommunication, drug delivery monitoring, and sensing applications. To investigate the ultrasound generation from the BT-PLGA transducer ( $\sim 200$   $\mu$ m thick), a continuous sinusoidal signals at different frequencies were applied to the 30 w/v% BT-PLGA transducer via a function generator and a power amplifier. The generated ultrasound was measured using a fiber optics hydrophone about 10 cm away from the transducer. Fig. 5(a) shows an FFT of the hydrophone response when the BT-PLGA was driven with 5.2 MHz sinusoidal waves. A clear peak corresponding to the driving frequency of 5.2 MHz is observed from the hydrophone output, confirming the inverse piezoelectric effect of the BT-PLGA. We ensured that the output was not due to another effect, such as the coupling between the fiber optics system and the RF amplifier, by replacing the BT-PLGA transducer with the PLGA-only sample. We observed no detectable signal (data not shown)

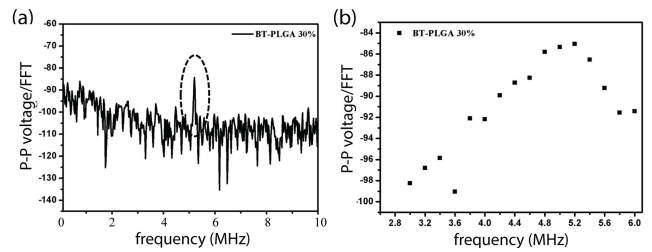


**FIGURE 5.** Piezoelectric ultrasonic transducer: (a) BT-PLGA transducer emitting ultrasonic waves with resonance frequency of 5.2 MHz when electrically stimulated using continuous sine wave at 250 mV pp (b) BT-PLGA transducer showing highest output voltage at its resonant frequency (5.2 MHz).

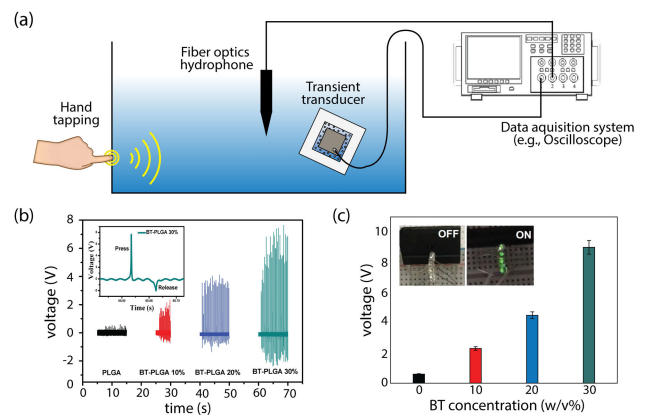


**FIGURE 6.** Energy harvesting from low frequency acoustic waves: (a) Experimental setup for energy harvesting, (b) open circuit voltage ( $V_{oc}$ ) of BT-PLGA transducers of different BT NPs concentration (0, 10, 20, 30% w/v) under the mechanical force (hand tapping); inset: enlarged image of a single peak-to-peak voltage graph of BT-PLGA transducer (30% w/v) under compression and relaxation (c) 2D graph depicting increase in piezoelectric output voltage of BT-PLGA transducer with increase in BT NPs concentration; inset: optical image of LED lit up using the piezoelectric potential generated from the device.

confirming that the hydrophone output is due to the generated ultrasound. To find the resonant frequency of the BT-PLGA ultrasonic transducer, it was electrically stimulated with continuous sinusoidal with frequencies ranging from 3 MHz to 6 MHz (Fig. 5(b)). From the frequency response of the BT-PLGA ultrasonic transducer, the resonant frequency was identified to be 5.2 MHz, which appeared to be linked to the thickness mode of the vibration. The calculated resonance frequency based on thickness mode (equ. 3) was 5.7 MHz, which agreed reasonably well with the experimental result (the speed of sound in PLGA was taken as 2300 m/s [37]).

$$f = \frac{SOS_{PLGA}}{2t_{PLGA}} \quad (3)$$

The demonstrated ability of the BT-PLGA transducer to exhibit both piezoelectric and inverse piezoelectric effect enables it to be bidirectional transducer, suitable for ultrasonic powering as well as for communication of vital biological information, potentially adding another functionality to transient diagnostic/therapeutic implants.

### C. LOW FREQUENCY ACOUSTIC WAVE ENERGY HARVESTING

In addition to the ultrasonic powering through the BT-PLGA transducer, we investigate the possibility of energy harvesting from low frequency acoustics generated within the body. While the low frequency acoustics may not be as intense as the externally applied ultrasound, they are more abundantly available from the human motions or ambient sounds, and thus can power the implant without the need of the external transducer [24], [38], [39]. Hence, we explore the energy harvesting from the low acoustic waves with BT-PLGA transducers as another mode of powering scheme.

The experimental setup is illustrated in Fig. 6(a). The setup was identical to that of ultrasonic powering, except the external transducer was now replaced by the hand tapping to generate low frequency vibrations. Hand tapping was applied at one end of the water tank about 10 cm away from the BT-PLGA transducer. A similar trend of increasing peak-to-peak  $V_{oc}$  was observed for low frequency acoustics harvesting as the output voltage monotonically increased with the increasing BT concentrations. Fig. 6(b) shows the time trace of the measured output voltage under low frequency waves generated by hand tapping. Although some voltage outputs were observed from the PLGA film ( $V_{pp}$  of 0.6 V), likely due to the capacitive effect, they were small compared to the voltage output of 30 w/v% BT-PLGA ( $V_{pp}$  of 9V). We attribute the large voltage output of the BT-PLGA transducer to the large pressure generated by the hand tapping. The force generated by the tapping with a finger was in the order of 10 N; assuming a contact area between a finger and the wall to be around 1 cm  $\times$  1 cm, the acoustic pressure of the low frequency waves were estimated to be in the order of 100 kPa. The low frequency acoustic pressure is more than an order of magnitude greater than the ultrasound used in ultrasonic powering (we note that this large acoustic pressure will rarely be generated naturally inside the body, but was used for demonstration purpose only). An enlarged image of single peak-to-peak voltage graph of BT-PLGA 30 % w/v transducer under compression and relaxation due to low frequency acoustics is given as inset in Fig. 6(b). The average  $V_{pp}$  generated from transducers with different BT concentrations are summarized in Fig. 6(c). Similar to the case of ultrasonic powering, both the concentration effect and the polling effect on the transducer output characteristics indicate that the piezoelectric effect is responsible for the energy harvesting. To demonstrate the feasibility of the powering small implants from low frequency acoustic waves, the BT-PLGA transducer was connected to a rectifier (GBJ25G, GeneSiC Semiconductor, USA) to convert the alternating electric current (AC) signal to direct current (DC). Four green LEDs (WP710A10LZGCK, Kingbright) were then connected in parallel to the output of the rectifier. Using the harvested energy from low frequency vibrations, the LEDs were readily powered on as shown in the inset of Fig. 6(c). Since the BT-PLGA is rigidly clamped to a support, the vibration mode of the transducer is also expected to be in the thickness mode along the direction of

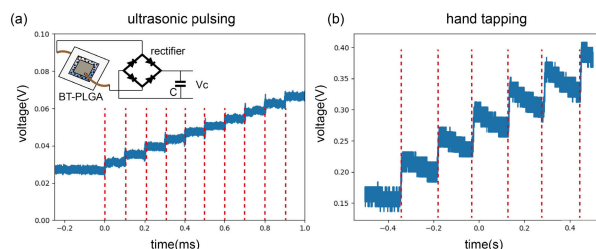


**FIGURE 7.** Capacitor charging performance of BT-PLGA: (a) The capacitor charging performance of BT-PLGA transducer with ultrasonic powering. Each red vertical dashed line indicates the arrival of the ultrasonic pulse. (inset: 30 w/v% BT-PLGA transducer is connected to a full-bridge rectifier connected to a 100 nF capacitor). (b) The capacitor charging performance of BT-PLGA transducer under low frequency acoustics generated from hand tapping.

the polarization, similar to the case of ultrasonic powering (Fig. 4a).

Since the harvested electrical energy is often stored in a capacitor, the transducer's ability to charge a capacitor is also critical in powering implants. Thus, we demonstrate the charging performance of the BT-PLGA transducer using two acoustic sources; ultrasound and low frequency acoustics. The BT-PLGA transducer was tested using the previously described setup (Fig. 4a and Fig. 6a) with one modification; the output of the transducer was connected to a full bridge rectifier and a 100 nF capacitor (Fig. 7a inset). The charge accumulation in the capacitor was monitored under ultrasonic irradiation (Fig. 7a) and low frequency vibration generated from hand tapping (Fig. 7b). The red vertical lines indicate the timings of the ultrasonic pulses and the low-frequency acoustics generated from hand tapping arriving at the BT-PLGA transducer surface. It can be seen that the voltage across the capacitor increases after each pulse whether it is from the ultrasound or low frequency vibrations (Fig. 7), confirming the charging capability of BT-PLGA.

### D. DEGRADATION PROCESS OF BT-PLGA TRANSDUCERS

Lastly, we examine the degradation of the biodegradable BT-PLGA transducer. To simulate the physiological conditions, PBS (pH of 7.4) was used as the degradation medium. The degradation process of BT-PLGA composite material appeared to be bulk erosion, by comparing Fig. 8a and Fig. 8b, which was consistent with the well-known bulk degradation behavior of PLGA [40]. The bulk erosion behavior of BT-PLGA is due to the fact that, in 0-3 composite, PLGA provides the structural integrity of the device; hence, the degradation of PLGA will naturally cause the embedded nanoparticles to be released from the film, similar to the drug delivery devices using biodegradable polymers [40]. Therefore, the degradation time and the degradation process (i.e. surface vs. bulk) of the 0-3 piezoelectric composite follows that of a PLGA film. The time scale of degradation was about 100 days; the structural integrity of the device was lost at  $\sim$ 50 days and a complete degradation of the whole device occurred at  $\sim$ 100 days as shown in Fig. 8 (a)-(c). The time

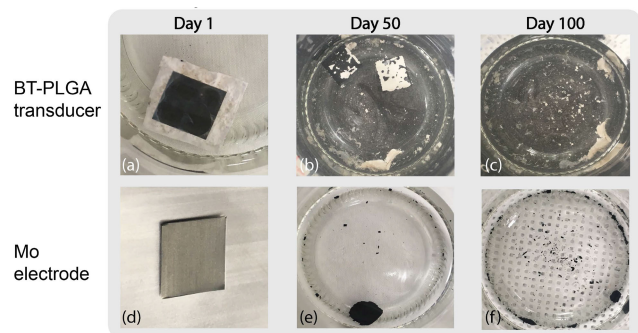


**FIGURE 8.** Degradation (0.1M PBS, pH = 7.4, and 37°C) of (a-c) BT-PLGA device (d-f) and MO electrode over a period of ~100 days.

scale for the complete degradation of Mo electrodes were similar at 37 ° (Fig. 8(d)-(f)). However, the degradation of the Mo sheets attached to the transducer appears to be slower than that in the case of standalone. This difference is attributed to the fact that one side of the electrode is protected from the environment by BT-PLGA composite. We expect that both BT-PLGA and Mo electrodes can be degraded at the same rate by reducing the thickness of the Mo electrode (we used ~ 25  $\mu\text{m}$  Mo electrode for this experiment).

Further, the functional period of the device is expected to be controlled through two parameters. Firstly, PLGA is known to have different degradation kinetics depending on the ratio between the lactic acid and glycolic acid [41]; thus, the functional period of the device can be controlled by modifying the composition of the biodegradable polymer, since the degradation kinetics of BT-PLGA follows that of PLGA. In addition, the total degradation time and the operation period both depend on the overall dimension of the device such as the thickness of the electrodes and encapsulating films.

### III. CONCLUSION

In summary, we developed and demonstrated a biodegradable piezoelectric transducer, which can potentially be utilized to power transient implants. The 0-3 composite of BT-PLGA based transducer is capable of generating upto 1  $\text{mW}/\text{cm}^2$  from ultrasonic powering and energy harvesting from low frequency acoustic waves. The traducer can also function as an ultrasonic transmitter for various applications. The entire device is biodegradable within 100 days; the degradation time can be tuned by modulating the composition of PLGA and thickness of Mo electrodes. To the best of our knowledge, this is the first demonstration of a biodegradable piezoelectric transducer that can possibly address the powering needs of the small deeply seated transient implants. Currently, however, the clearance of BT nanoparticles remains a concern; while BT is known to be biocompatible, the cytotoxicity of nanoparticles at relatively high concentration can be a possible issue. In addition, despite the large maximum power harvesting demonstrated in this work, the energy density is relatively modest. Despite these limitations, for a deeply seated small implants, even a device with an active area of 1  $\text{mm} \times 1 \text{mm}$

can harvest upto 100  $\mu\text{W}$  under intense ultrasonic irradiation, enough to operate a low power IC circuitry.

### REFERENCES

- [1] S. Lee, J. Koo, S.-K. Kang, G. Park, Y. J. Lee, Y.-Y. Chen, S. A. Lim, K.-M. Lee, and J. A. Rogers, "Metal microparticle—Polymer composites as printable, bio/ecoresorbable conductive inks," *Mater. Today*, vol. 21, no. 3, pp. 207–215, Apr. 2018.
- [2] K. K. Fu, Z. Wang, J. Dai, M. Carter, and L. Hu, "Transient electronics: Materials and devices," *Chem. Mater.*, vol. 28, no. 11, pp. 3527–3539, Jun. 2016.
- [3] K. J. Yu, D. Kuzum, S.-W. Hwang, B. H. Kim, H. Juul, N. H. Kim, S. M. Won, K. Chiang, M. Trumpis, and A. G. Richardson, "Bioresorbable silicon electronics for transient spatiotemporal mapping of electrical activity from the cerebral cortex," *Nature Mater.*, vol. 15, no. 7, pp. 782–791, Jul. 2016.
- [4] Y. Gao, Y. Zhang, X. Wang, K. Sim, J. Liu, J. Chen, X. Feng, H. Xu, and C. Yu, "Moisture-triggered physically transient electronics," *Sci. Adv.*, vol. 3, no. 9, Sep. 2017, Art. no. e1701222.
- [5] L. Yin, X. Huang, H. Xu, Y. Zhang, J. Lam, J. Cheng, and J. A. Rogers, "Materials, designs, and operational characteristics for fully biodegradable primary batteries," *Adv. Mater.*, vol. 26, no. 23, pp. 3879–3884, Jun. 2014.
- [6] J.-K. Chang, H.-P. Chang, Q. Guo, J. Koo, C.-I. Wu, and J. A. Rogers, "Biodegradable electronic systems in 3D, heterogeneously integrated formats," *Adv. Mater.*, vol. 30, no. 11, Mar. 2018, Art. no. 1704955.
- [7] E. J. Curry, K. Ke, M. T. Chorsi, K. S. Wrobel, A. N. Miller, A. Patel, I. Kim, J. Feng, L. Yue, and Q. Wu, "Biodegradable piezoelectric force sensor," *Proc. Nat. Acad. Sci. USA*, vol. 115, no. 5, pp. 909–914, 2018.
- [8] J. Koo, M. R. MacEwan, S.-K. Kang, S. M. Won, M. Stephen, P. Gamble, Z. Xie, Y. Yan, Y.-Y. Chen, and J. Shin, "Wireless bioresorbable electronic system enables sustained nonpharmacological neuroregenerative therapy," *Nature Med.*, vol. 24, no. 12, pp. 1830–1836, Dec. 2018.
- [9] D.-H. Kim, J. Viventi, J. J. Amsden, J. Xiao, L. Vigeland, Y.-S. Kim, J. A. Blanco, B. Panilaitis, E. S. Frechette, D. Contreras, D. L. Kaplan, F. G. Omenetto, Y. Huang, K.-C. Hwang, M. R. Zakin, B. Litt, and J. A. Rogers, "Dissolvable films of silk fibroin for ultrathin conformal bio-integrated electronics," *Nature Mater.*, vol. 9, no. 6, pp. 511–517, Jun. 2010.
- [10] F. Patolsky and C. M. Lieber, "Nanowire nanosensors," *Mater. Today*, vol. 8, no. 4, pp. 20–28, Apr. 2005.
- [11] S.-W. Hwang, C. H. Lee, H. Cheng, J.-W. Jeong, S.-K. Kang, J.-H. Kim, J. Shin, J. Yang, Z. Liu, G. A. Ameer, Y. Huang, and J. A. Rogers, "Biodegradable elastomers and silicon Nanomembranes/Nanoribbons for stretchable, transient electronics, and biosensors," *Nano Lett.*, vol. 15, no. 5, pp. 2801–2808, May 2015.
- [12] C.-H. Wang, C.-Y. Hsieh, and J.-C. Hwang, "Flexible organic thin-film transistors with silk fibroin as the gate dielectric," *Adv. Mater.*, vol. 23, no. 14, pp. 1630–1634, Apr. 2011.
- [13] S.-W. Hwang, J.-K. Song, X. Huang, H. Cheng, S.-K. Kang, B. H. Kim, J.-H. Kim, S. Yu, Y. Huang, and J. A. Rogers, "High-performance Biodegradable/Transient electronics on biodegradable polymers," *Adv. Mater.*, vol. 26, no. 23, pp. 3905–3911, Jun. 2014.
- [14] S.-W. Hwang, H. Tao, D.-H. Kim, H. Cheng, J.-K. Song, E. Rill, M. A. Brenckle, B. Panilaitis, S. M. Won, and Y.-S. Kim, "A physically transient form of silicon electronics," *Science*, vol. 337, no. 6102, pp. 1640–1644, Sep. 2012.
- [15] Q. Zheng, Y. Zou, Y. Zhang, Z. Liu, B. Shi, X. Wang, Y. Jin, H. Ouyang, Z. Li, and Z. L. Wang, "Biodegradable triboelectric nanogenerator as a life-time designed implantable power source," *Sci. Adv.*, vol. 2, no. 3, Mar. 2016, Art. no. e1501478.
- [16] M. A. Hannan, S. Mutashar, S. A. Samad, and A. Hussain, "Energy harvesting for the implantable biomedical devices: Issues and challenges," *Biomed. Eng. OnLine*, vol. 13, no. 1, p. 79, 2014.
- [17] D. C. Bock, A. C. Marschilok, K. J. Takeuchi, and E. S. Takeuchi, "Batteries used to power implantable biomedical devices," *Electrochimica Acta*, vol. 84, pp. 155–164, Dec. 2012.
- [18] B. B. Owens, *Batteries for Implantable Biomedical Devices*. Berlin, Germany: Springer, 2012.
- [19] S. Kerzenmacher, J. Ducreé, R. Zengerle, and F. von Stetten, "Energy harvesting by implantable abiotically catalyzed glucose fuel cells," *J. Power Sour.*, vol. 182, no. 1, pp. 1–17, Jul. 2008.

- [20] W. Jiang, H. Li, Z. Liu, Z. Li, J. Tian, B. Shi, Y. Zou, H. Ouyang, C. Zhao, L. Zhao, R. Sun, H. Zheng, Y. Fan, Z. L. Wang, and Z. Li, "Fully bioabsorbable natural-materials-based triboelectric nanogenerators," *Adv. Mater.*, vol. 30, no. 32, Aug. 2018, Art. no. 1801895.
- [21] Z. Li, H. Feng, Q. Zheng, H. Li, C. Zhao, H. Ouyang, S. Noreen, M. Yu, F. Su, R. Liu, L. Li, Z. L. Wang, and Z. Li, "Photothermally tunable biodegradation of implantable triboelectric nanogenerators for tissue repairing," *Nano Energy*, vol. 54, pp. 390–399, Dec. 2018.
- [22] H. Li, C. Zhao, X. Wang, J. Meng, Y. Zou, S. Noreen, L. Zhao, Z. Liu, H. Ouyang, P. Tan, M., Y. Fan, Z. L. Wang, and Z. Li, "Fully bioabsorbable capacitor as an energy storage unit for implantable medical electronics," *Adv. Sci.*, vol. 6, no. 6, Mar. 2019, Art. no. 1801625.
- [23] G. Lee, S.-K. Kang, S. M. Won, P. Gutruf, Y. R. Jeong, J. Koo, S.-S. Lee, J. A. Rogers, and J. S. Ha, "Fully biodegradable microsupercapacitor for power storage in transient electronics," *Adv. Energy Mater.*, vol. 7, no. 18, Sep. 2017, Art. no. 1700157.
- [24] R. Hinchet, H.-J. Yoon, H. Ryu, M.-K. Kim, E.-K. Choi, D.-S. Kim, and S.-W. Kim, "Transcutaneous ultrasound energy harvesting using capacitive triboelectric technology," *Science*, vol. 365, no. 6452, pp. 491–494, Aug. 2019.
- [25] A. Sanni and A. Vilches, "Powering low-power implants using PZT transducer discs operated in the radial mode," *Smart Mater. Struct.*, vol. 22, no. 11, Nov. 2013, Art. no. 115005.
- [26] H. Basaeri, D. B. Christensen, and S. Roundy, "A review of acoustic power transfer for bio-medical implants," *Smart Mater. Struct.*, vol. 25, no. 12, Dec. 2016, Art. no. 123001.
- [27] D. L. Miller, N. B. Smith, M. R. Bailey, G. J. Czarnota, K. Hynynen, and I. R. S. Makin, "Overview of therapeutic ultrasound applications and safety considerations," *J. Ultrasound Med.*, vol. 31, no. 4, pp. 623–634, Apr. 2012.
- [28] S. H. Song, A. Kim, and B. Ziaie, "Omnidirectional ultrasonic powering for millimeter-scale implantable devices," *IEEE Trans. Biomed. Eng.*, vol. 62, no. 11, pp. 2717–2723, Nov. 2015.
- [29] A. Denisov and E. Yeatman, "Ultrasonic vs. inductive power delivery for miniature biomedical implants," in *Proc. Int. Conf. Body Sensor Netw.*, Jun. 2010, pp. 84–89.
- [30] Z.-H. Lin, Y. Yang, J. M. Wu, Y. Liu, F. Zhang, and Z. L. Wang, "BaTiO<sub>3</sub> nanotubes-based flexible and transparent nanogenerators," *J. Phys. Chem. Lett.*, vol. 3, no. 23, pp. 3599–3604, Dec. 2012.
- [31] H. Fu and R. E. Cohen, "Polarization rotation mechanism for ultrahigh electromechanical response in single-crystal piezoelectrics," *Nature*, vol. 403, no. 6767, pp. 281–283, Jan. 2000.
- [32] S. Selvarajan, N. R. Alluri, A. Chandrasekhar, and S.-J. Kim, "Direct detection of cysteine using functionalized BaTiO<sub>3</sub> nanoparticles film based self-powered biosensor," *Biosensors Bioelectron.*, vol. 91, pp. 203–210, May 2017.
- [33] M. A. Wood and K. A. Ellenbogen, "Cardiac pacemakers from the patient's perspective," *Circulation*, vol. 105, no. 18, pp. 2136–2138, 2002.
- [34] R. E. Newnham, L. J. Bowen, K. A. Klicker, and L. E. Cross, "Composite piezoelectric transducers," *Mater. Des.*, vol. 2, pp. 93–106, Dec. 1980.
- [35] H. Lee, S. Zhang, Y. Bar-Cohen, and S. Sherrit, "High temperature, high power piezoelectric composite transducers," *Sensors*, vol. 14, no. 8, pp. 14526–14552, 2014.
- [36] H. Hayashi, T. Nakamura, and T. Ebina, "In-situ Raman spectroscopy of BaTiO<sub>3</sub> particles for tetragonal–cubic transformation," *J. Phys. Chem. Solids*, vol. 74, no. 7, pp. 957–962, Jul. 2013.
- [37] N. Parker, M. Mather, S. Morgan, and M. Povey, "Longitudinal acoustic properties of poly (lactic acid) and poly (lactic-co-glycolic acid)," *Biomed. Mater.*, vol. 5, no. 5, 2010, Art. no. 055004.
- [38] S. Kim, S. J. Choi, K. Zhao, H. Yang, G. Gobbi, S. Zhang, and J. Li, "Electrochemically driven mechanical energy harvesting," *Nature Commun.*, vol. 7, no. 1, p. 10146, Apr. 2016.
- [39] S. Roundy and P. K. Wright, "A piezoelectric vibration based generator for wireless electronics," *Smart Mater. Struct.*, vol. 13, no. 5, pp. 1131–1142, Oct. 2004.
- [40] F. V. Burkersroda, L. Schedl, and A. Göpferich, "Why degradable polymers undergo surface erosion or bulk erosion," *Biomaterials*, vol. 23, no. 21, pp. 4221–4231, Nov. 2002.
- [41] T. G. Park, "Degradation of poly(lactic-co-glycolic acid) microspheres: Effect of copolymer composition," *Biomaterials*, vol. 16, no. 15, pp. 1123–1130, Oct. 1995.



**SOPHIA SELVARAJAN** received the B.S. degree in biotechnology from Tamil Nadu Agricultural University, in 2011, the M.S. degree in nanotechnology from Karunya University, in 2013, and the Ph.D. degree in advanced convergence technology and science; nanobiotechnology from Jeju National University, Jeju, South Korea, in 2018.

From 2018 to 2019, she was a Postdoctoral Researcher with the Electronics Engineering Department, Sookmyung Women's University, Seoul, South Korea. Since 2019, she has been a Postdoctoral Researcher with the Department of Biophysics, Institute of Quantum Biophysics (IQB), Sungkyunkwan University (SKKU), Suwon, South Korea.



**ALBERT KIM** (Member, IEEE) received the B.S., M.S., and Ph.D. degrees in electrical and computer engineering from Purdue University, West Lafayette, IN, USA, in 2008, 2011, and 2015, respectively.

He joined Intel Corporation as a Research and Development Engineer, from 2015 to 2017, before coming back to academia. He is currently an Assistant Professor with the Department of Electrical and Computer Engineering, Temple University, Philadelphia, PA, USA.



**SEUNG HYUN SONG** received the B.S. degree in electrical engineering from Iowa State University, Ames, IA, USA, in 2009, and the Ph.D. degree from Purdue University, West Lafayette, IN, USA, in 2014.

From 2014 to 2018, he was a Postdoctoral Researcher with the Center for Integrated Nanostructures and Physics (CINAP), Sungkyunkwan University, Suwon, South Korea. Since 2018, he has been an Assistant Professor with the Department of Electronics Engineering, Sookmyung Women's University, Seoul, South Korea.

• • •